ELSEVIER

Journal of Photochemistry and Photobiology A: Chemistry 105 (1997) 129–134

Journal of PHOTOCHEMISTRY AND PHOTOBIOLOGY A:CHEMISTRY

The dynamics of azulene S_2 state characterised by femtosecond transient absorption spectroscopy

Lorenzo Ciano [a,b], Paolo Foggi [a,b,*], Pier Remigio Salvi [a,b]

[a] *LENS, Largo E. Fermi 2, 50125 Firenze, Italy*

[b] *Dipartimento di Chimica, via G. Capponi 9, 50121 Firenze, Italy*

Received 15 July 1996; accepted 11 December 1996

Abstract

The fast dynamics of the population build-up of S_2 state of azulene in ethylene glycol and the following relaxation processes are investigated by transient absorption spectroscopy. The transient spectrum shows bands at 469, 413 and 366 nm. The spectral data are compared to the results of semi-empirical calculations based on the QCFF/PI method. The build-up of S_2 population is measured by following the growth in intensity of the main peak (366 nm) as the function of the delay between the pump (340 nm) and the probe (broad continuum). The experimental points are fitted by a single exponential curve with time constant of 300 ± 50 fs. The process is dominated by the fast motions of the solvent cage. The decay of the state occurs with a single exponential mechanism with time constant of 1.06 ± 0.03 ns. © 1997 Elsevier Science S.A.

Keywords: Excited state dynamics; Electronic dephasing; Transient spectroscopy

1. Introduction

Azulene (Fig. 1) is the most investigated among the known examples of closed-shell polyatomic molecules exhibiting $S_0 \leftarrow S_2$ fluorescence [1]. It has been the subject of extensive theoretical and experimental studies. In recent years the dynamics of S_1 and S_2 states have been characterised by time-resolved techniques. Several pump–probe experiments with sub-picosecond resolution have been performed to measure the lifetime of the short lived S_1 state in solution [2–7]. The S_2 lifetime and fluorescence quantum yield have been measured and correlated to the energy gap between S_2, S_1 and related triplet states [8]. Many calculations have been done in order to give a correct interpretation of ground state spectral data (frequencies and intensities), and other properties of the first excited states [9–12].

In this paper we present preliminary results obtained by measuring the transient absorption spectrum from S_2 state. Transient absorption spectroscopy with a broad band probe is a unique tool because it contains both spectral and dynamical information [13–15]. It provides simultaneously the energy of the transition starting from a particularly prepared excited state and the dynamics of formation and decay of this state. In addition, wavelength shifts of the peak maxima occurring in the first picosecond after excitation can provide more details than the simple evolution of the transient absorption at fixed wavelength. The observation of the growth and disappearance of the bands provides a complete description of the dynamics of excited states. Furthermore the observation of transitions to energy levels otherwise not observable in classical absorption spectroscopy is feasible because of different symmetry selection rules and the possibility to attain very high excitation energy up to the VUV spectral region.

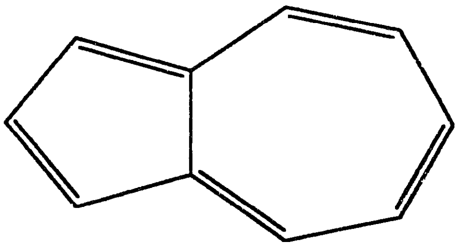

Fig. 1. Molecular structure of azulene.

We report on the observation of some effects due to ultrafast dynamics occurring in the S_2 state after excitation and on the slower dynamics of population decay from the same state. The latter results are compared with those obtained by time resolved fluorescence spectroscopy.

---

[*] Corresponding author. Tel.: +39-55 2307818; fax: +39-55-224072; e-mail: foggi@lens.unifi.it.

PII S1010-6030(96)04606-0

2. Experimental and data handling

The femtosecond laser system utilised in the present experiment has been described in previous papers [16,17]. Briefly, a titanium sapphire laser (Spectra Physics Tsunami) able to provide 70 fs (FWHM) pulses at 800 nm is amplified at 1 kHz by a regenerative amplifier (BMI Alpha 1000) pumped by a intracavity frequency doubled Nd:YLF (BMI 621-D). The amplified pulses (typical energy 800 μJ per pulse and duration 120 fs) is used to pump a travelling wave parametric generator tunable in the 1.2–2.4 μm range [18]. The output (signal + idler) has an average power of about 250 μJ (>25% conversion). In the present experiment the signal pulse (150 μJ and 80 fs at 1.36 mm) is doubled twice in two thin BBO crystals to achieve pulses in the UV at 340 nm (3–5 μJ and 80 fs) [19] at the maximum of $S_2 \leftarrow S_0$ transition of the absorption spectrum in ethylene glycol (see Fig. 2). A small portion of the amplified train (5 μJ) is split off before the parametric generator and focused, after passing through a delay line, into a 2 mm thick CaF_2 plate. In this way a broad white continuum (290–700 nm) is obtained. The components of the continuum are time-dispersed, owing to the dispersion of the linear and non linear refraction indices in the CaF_2 plate itself. The temporal behaviour of the probe has been characterised: the total dispersion is 1.5 ps between the wavelength limits and 1 ps between 290 and 450 nm components. Several spectra have been recorded at close intervals (30 fs) and then reconstructed in order to recover the dispersion within 200 fs. The cross correlation between the continuum and the excitation pulses has been measured by looking at the stimulated Raman gain intensity of the CH stretching band of dodecane in a jet and was found to have a gaussian shape with a duration of 200 fs (FWHM). The UV and the continuum pulses, linearly polarised at 0° and 54.7° respectively, are focused by a parabolic mirror onto the sample. In order to reduce the noise due to thermal fluctuations, the sample (azulene solution 5×10^{-3} M in ethylene glycol) is flowed through a 400 μm jet. This method has two limitations: firstly, only solutions with viscous solvents can provide stable jets and secondly, oxygen cannot be completely removed from the solution.

Probe and reference beams are focused with a cylindrical lens onto the entrance slit of a flat field spectrograph. Two images deriving from the probe and the reference are selected on the CCD detector. The ratio between their intensities provides the transient transmittance of the solution. Each spectrum is collected over 4 min, corresponding to 240 000 laser shots. In this way it is possible to observe transmittance variations of the order of 0.5%.

3. Results and discussion

In Fig. 3 the transient spectra recorded 2 ps and 16 ps after excitation are reported. The spectra are corrected for the dispersion of the white continuum, as described in the previous section, and for the presence of fluorescence peaks, by subtracting spectra recorded with the pump only from the spectra recorded with pump, probe and reference together. In Fig. 4 the build-up of the absorbance measured at the main peak wavelength at 363 nm is reported as a function of the delay between pump and probe.

Compensating for both the contribution of the spike and convolution with the instrumental function, the rise time is 300 ± 50 fs. The fitting has been performed with a program, based on Powell's method, which includes the convolution of the molecular response with the instrumental function [14]. The signal $S(t)$ is given by

$$S(t) = \int dt\, F(t-\tau)R(t) \qquad (1)$$

where $F(t)$ is the instrumental function measured according to the procedure described in the previous section and $R(t)$ is the molecular response function:

$$R(t) = W_1\delta(t) + W_2(1-e^{-t/\tau})H(t) \qquad (2)$$

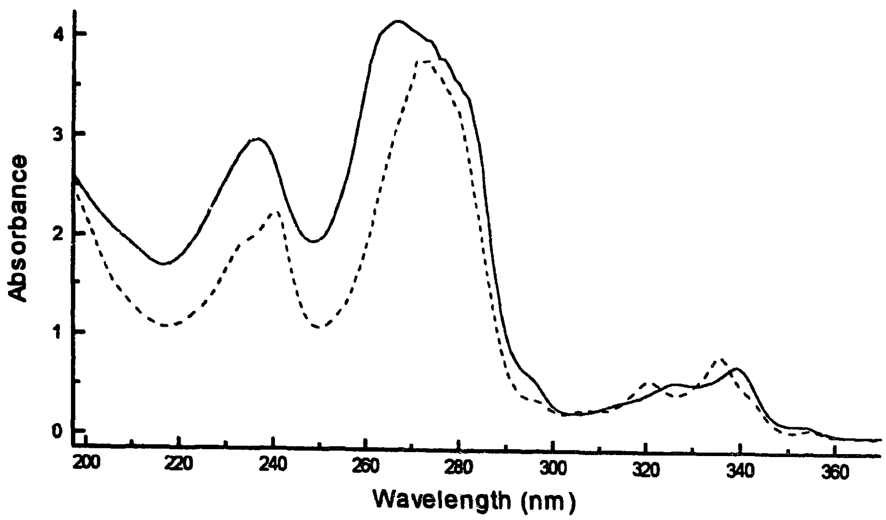

Fig. 2. The absorption spectra of azulene in cyclohexane (dashed line) and ethylene glycol (solid line).

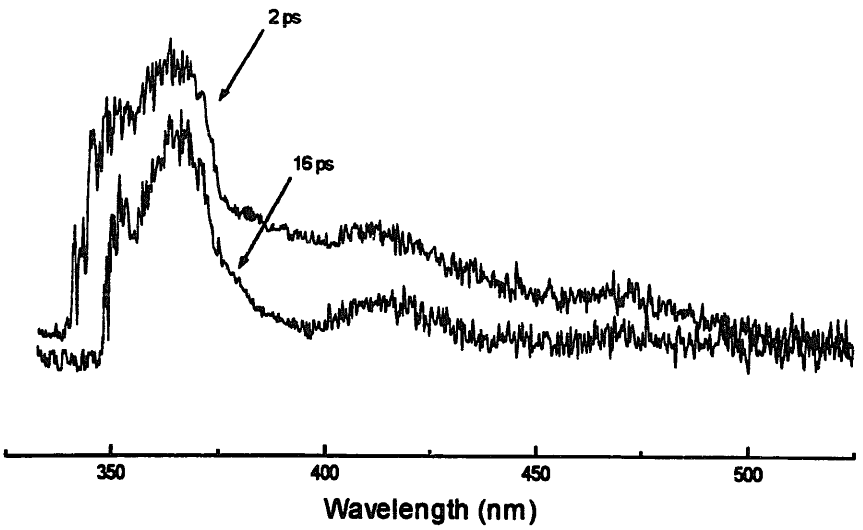

Fig. 3. Transient absorption spectrum of azulene in solution recorded 2 ps (upper line) and 16 ps (lower line) after excitation at 340 nm.

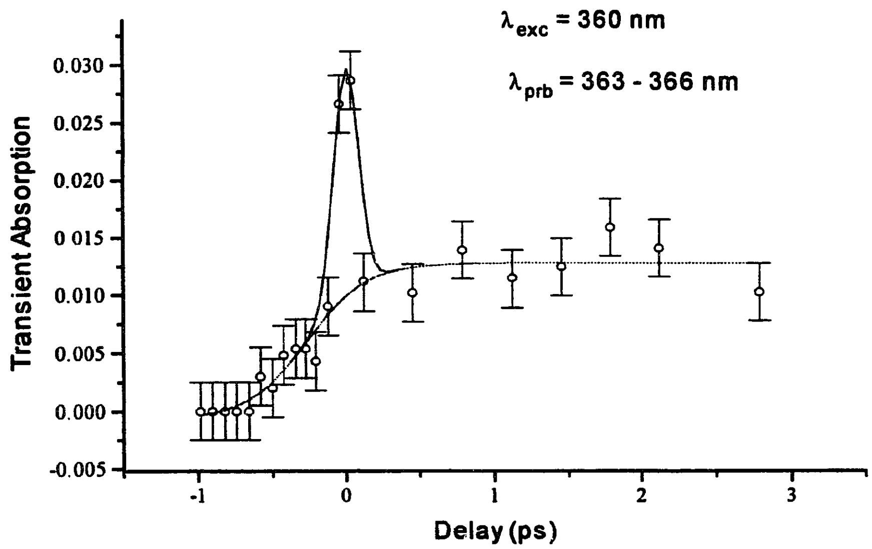

Fig. 4. Time evolution of the transient absorption of azulene in solution.

where the Ws are the weights of the two contributions, τ is the time constant of the population formation process and $H(t)$ is the unitary step function.

Owing to the complexity of the evolution of transient absorption spectra a detailed discussion is required. Therefore we divide the analysis of the results into three parts. The first one discusses the fast evolution of the transient in the first few picoseconds. The second one deals with the slower relaxation dynamics and in the third part we discuss the transient spectrum of the relaxed S_2 state and we compare the experimental data with the results of semi-empirical calculations.

3.1. *The fast dynamics*

The evolution of the various spectral features appearing in the transient spectra after excitation of S_2 state must be discussed taking into account the following observations.

1. The excitation wavelength is at 340 nm.
2. The main peak in the transient is at 366 nm.
3. The maximum of the fluorescence spectrum from S_2 state is at 377 nm.

Within 40 nm we have the occurrence of three distinct processes which can interact to produce more complex signals (see Fig. 5). In the light of the above mentioned points we can give an explanation of the fast changes observed in the transient spectra which can be summarised as follows.

1. The central peak position moves from shorter (359 nm) to longer (366 nm) wavelengths. The latter value is then observed in the spectra recorded at longer delays. The overall effect occurs in about 300 fs.
2. Around zero delay time an intensification of transient absorbance is observed together with stimulated emission.
3. From the analysis of the transient absorbance the rise time of population formation in S_2 state results to be 300±50 fs.

Points 1 and 2 can be interpreted as processes due to the fast relaxation dynamics involving the solvent cage around the molecule. It is well known that all solvents, independently of

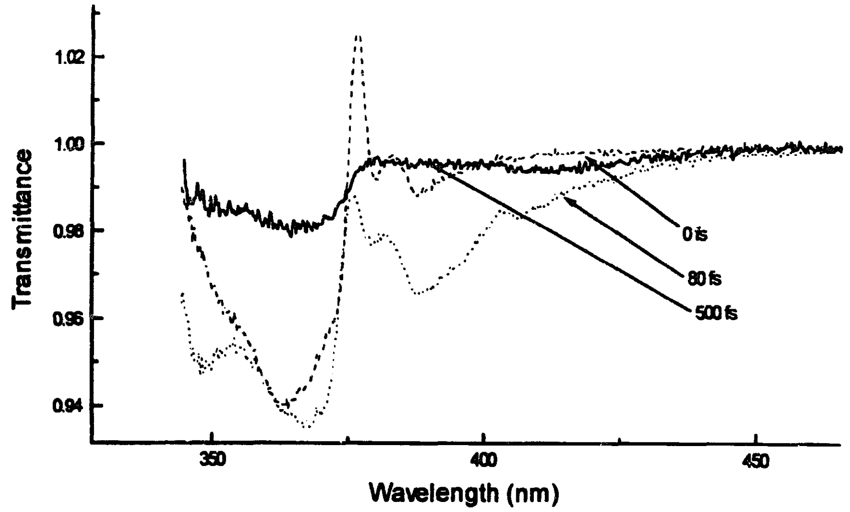

Fig. 5. The evolution of the transmittance during the first 0.5 ps. When pump and probe are overlapped (0 and 80 fs curves) a strong absorption around 360 nm is observed together with the stimulated emission at 377 and 383 nm. When the pulses are well separated (500 fs curve) the regular absorption features are observed.

their viscosity, possess femtosecond non-diffusive inertial relaxation. The fast relaxation time for ethylene glycol has been measured, by time resolved optical Kerr effect, to be of the order of 600 fs [20]. The order of magnitude of the time constant for this process is the same as that observed in the present experiment. This interpretation is also consistent with the fact that the dephasing process, occurring in the excited state, is driven by the fast changes in the coordination of the solute molecule. The population build-up of the excited state must occur on the same time scale. This provides an explanation of the difference between the rise time measured in the present experiment and the dephasing time measured for azulene in cyclohexane, which is ten time shorter [2].

With regard to point 2, we observe that the intensification of the signal at zero delay time occurs along with strong fluorescence. The latter cannot be eliminated by the subtraction procedure previously mentioned and consequently is interpreted as resulting from stimulated emission. Such intensification, which is the origin of the spike appearing in Fig. 4, may be attributed to the superposition of the transient electronic signal with an overdamped oscillation which probably occurs in both the ground and excited state. The limited time resolution of the present experiment does not allow the observation of any oscillatory behaviour such as has been reported in other experiments [21,22].

3.2. The slow decay dynamics

In Fig. 6 the comparison between the fluorescence decay (solid line) and the decay of transient absorbance (open

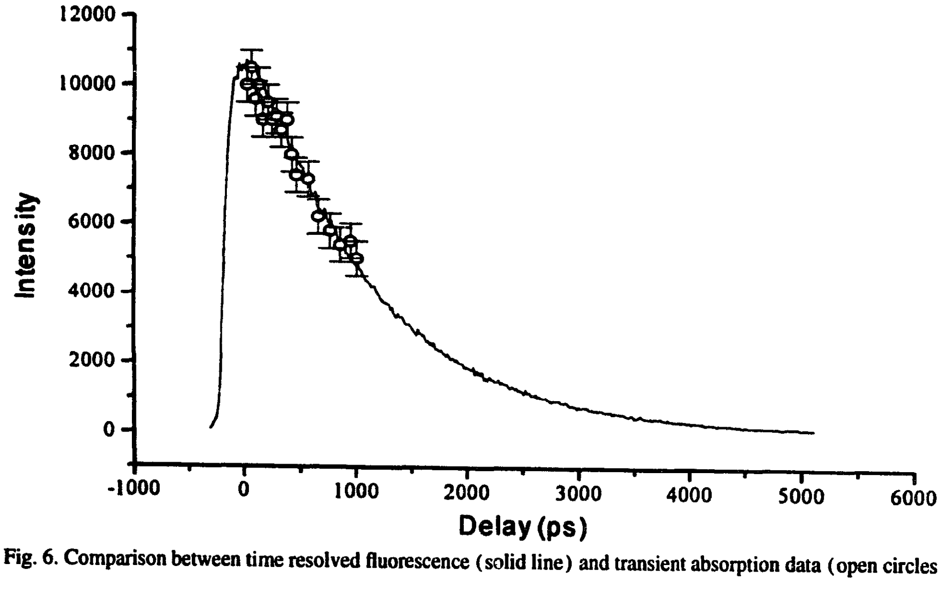

Fig. 6. Comparison between time resolved fluorescence (solid line) and transient absorption data (open circles).

Table 1
Experimental and calculated transition wavelengths of transient absorption spectrum from azulene S_2 state

	Experiment (nm) [a]	QCFF/PICIS (nm)	Corrected QCFF/PICIS (nm) [b]	Oscillator strength	Final state symmetry
$S_2 \rightarrow S_5$		598	617	0.0028	b_2
$S_2 \rightarrow S_6$	469	487	497	0.2673	a_1
$S_2 \rightarrow S_7$	413	429	434	0.1581	b_2
$S_2 \rightarrow S_8$		405	405	0.0044	a_1
$S_2 \rightarrow S_9$		373	379	0.0689	b_2
$S_2 \rightarrow S_{10}$	366 (353)	360	383	0.2405	a_1

[a] Present work.
[b] Difference between S_n and S_m energy levels corrected by zero-point vibrational energy (see text).

circles) is reported. The transient absorption measurements are limited by the length of our delay line, however the agreement between the two results is good. The decay constant obtained by fitting present data with a single exponential is 1.06 ± 0.03 ns. This is shorter than those obtained by time resolved fluorescence in various solvents. For example the fluorescence decay time of azulene in cyclohexane is 1.33 ns and in ethanol 1.31 ns [8]. This discrepancy may be attributed to the presence of oxygen in the solution and further measurements are needed to clarify this point. However the present experiment demonstrate the equivalence of transient absorption and time resolved fluorescence techniques.

3.3. *The transient spectrum*

As mentioned in Section 1, transient spectra also provide information about high energy molecular states not observable with other spectroscopic techniques [14]. In the present case we have been able to observe electronic transitions up to 60 000 cm^{-1} above the ground state. Bands appearing at such a high energy level could also be attributed to cation formation following multiphoton ionization of the molecule. If this was the case, a different time constant for the decay of the transient signal compared to that of fluorescence would be expected. This is not the case and therefore the main features of the transient spectrum are attributed to a $S_n \leftarrow S_2$ transitions.

This study has been completed by performing semi-empirical MO calculations on azulene within the QCFF/PI approximation and including single excitation configuration interaction [23]. This procedure is particularly suitable for the interpretation of the transient spectrum because it gives vertical excitation energies of optimized electronic states. The program has also been applied to calculate oscillator strengths of $S_n \leftarrow S_m$ in addition to $S_n \leftarrow S_0$ transitions. The results are summarised in Table 1. A good overall agreement with experiment is found. The number of excited states higher than S_2 in the range 600–350 nm with sufficiently high oscillator strength is equal to the observed transient band. Also, calculated vertical transition energies from optimised S_2 state satisfactorily agree with experiment. It is finally concluded, considering the difference between vertical and (0–0) transitions energies, that transient absorption probes in the present case the vibronic manifold of higher electronic states.

Acknowledgements

This work has been supported by the Commission of the European Communities under the contract n.GE1*CT 920046. Authors wish to thank Dr P. Bartolini for the help in performing fluorescence decay measurements. Authors acknowledge the contribution of R. Ballerini, M. Giuntini and M. DePas of the LENS technical staff in setting up the transient absorption experimental apparatus.

References

[1] M. Beer, H.C. Longuet-Higgins, J. Chem. Phys. 23 (1955) 1390.
[2] E.T.J. Nibbering, K.Duppen, D.A. Wiersma, J. Chem. Phys. 93 (1990) 5477.
[3] D. Schwarzer, J. Troe, J. Schroeder, Ber. Bunsenges. Phys. Chem. 95 (1991) 933.
[4] B.D. Wagner, M. Szymanski, R.P. Steer, J. Chem. Phys. 98 (1993) 301.
[5] D. Tittlebach-Helmrich, B.D. Wagner, R.P. Steer, Chem. Phys. Lett. 209 (1993) 464.
[6] T-S. Yang, R. Zhang, A.B. Myers, J. Chem. Phys. 100 (1994) 8573.
[7] D. Tittlebach-Helmrich, B.D. Wagner, R.P. Steer, Can. J. Chem. 73 (1995) 303.
[8] B.D. Wagner, D. Tittlebach-Helmrich, R.P. Steer, J. Phys. Chem. 96 (1992) 7904.
[9] F. Zerbetto, M.Z. Zgierski, Chem. Phys. 110 (1986) 421.
[10] F. Negri, M.Z. Zgierski, J. Chem. Phys. 99 (1993) 4318.
[11] P.M. Kozlowski, G. Rauhut, P. Pulay, J. Chem. Phys. 103 (1995) 5650.
[12] M.J. Bearpark, F. Bernardi, S. Clifford, M. Olivucci, M.A. Robb, B.R. Smith, T. Vreven, J. Am. Chem. Soc. 118 (1996) 169.
[13] G.R. Fleming, Chemical Application of Ultrafast Spectroscopy, Oxford University Press, New York, 1986.
[14] P. Foggi, L. Pettini, I. Sànta, R. Righini, S. Califano, J. Phys. Chem., 99 (1995) 7439.
[15] W. Thomas Pollard, R.A. Mathies, Annu. Rev. Phys. Chem. 43 (1992) 497.
[16] P. DiTrapani, A. Andreoni, P. Foggi, C. Solcia, R. Danielius, A. Piskarskas, Opt. Commun. 119 (1995) 327.

[17] C. de Lisio, C. Altucci, R. Bruzzese, S. Solimeno, F. Vigilante, M. Bellini, P. Foggi, Opt. Commun. 121 (1995) 73.

[18] I.M. Bayanov, R. Danielius, P. Heinz, A. Seilmeier, Opt. Commun. 113 (1994) 99.

[19] R. Danielius, A. Piskarskas, P. Di Trapani, A. Andreoni, C. Solcia, P. Foggi, Appl. Opt. 35 (1996) 5336.

[20] Y.J. Chang, E.W. Castner Jr., J. Chem. Phys. 99 (1993) 7289.

[21] K. Wynne, C. Galli, P.J.F. DeRege, M.J. Therien, R.M. Hochstrasser, in: Ultrafast Phenomena VIII. Proceedings of the 8th International Conference, Springer, Berlin, 1993, p. 71.

[22] M.H. Vos, F. Rapport, J.C. Lambry, J. Breton, J.L. Martin, Nature 363 (1993) 320.

[23] N.H. Warshell, M. Karplus, J. Am. Chem. Soc. 94 (1972) 5612.